Korean J. Chem. Eng., 40(7), 1606-1615 (2023)
DOI: 10.1007/s11814-023-1441-z

pISSN: 0256-1115
eISSN: 1975-7220

Pt substitution in Pd/Rh three-way catalyst for improved emission control

Do Yeong Kim*,‡, Wo Bin Bae*,‡, Sang Woo Byun*, Young Jin Kim, Dal Young Yoon***, Changho Jung***, Chang Hwan Kim***, Dohyung Kang****,†, Melanie J. Hazlett*****,†, and Sung Bong Kang*,†**

*Research Center for Innovative Energy and Carbon Optimized Synthesis for Chemicals (Inn-ECOSysChem) and School of Earth Sciences and Environmental Engineering, Gwangju Institute of Science and Technology, 123 Cheomdangwagi-ro, Gwangju 61005, Korea
**Center for Environment & Sustainable Resources, Korea Research Institute of Chemical Technology (KRICT), 141 Gajeong-ro, Daejeon 34114, Korea
***Energy & Environmental Chemical Systems Lab, IFAT (Institute of Fundamental & Advanced Technology), R&D Division, Hyundai Motor Company, 37, Cheoldobagmulgwan-ro, Uiwang-si, Gyeonggi-do 16082, Korea
****Department of Future Energy Convergence, Seoul National University of Science and Technology, 232 Gongreung-ro, Nowon-gu, Seoul 01811, Korea
*****Chemical and Materials Engineering, Gina Cody School of Engineering and Computer Science, Concordia University, Montreal, QC, H4B1R6, Canada
(*Received 10 December 2022 • Revised 8 February 2023 • Accepted 9 February 2023*)

Abstract−Gasoline engine vehicle emissions, such as nitrogen oxides (NO_x), CO and hydrocarbons (HCs), are a major source of air pollution, and require improved emission control systems. By-product NH_3 and N_2O emissions, which come from low N_2 selectivity in the emission control system, are also a major concern. The current study has comprehensively investigated the impact of the Pt-substitution in commercial Pd/Rh-based three-way catalyst (TWC) formulations with respect to catalytic performance. TWC performance was systematically evaluated with respect to the warm-up catalytic converter (WCC) and the under-floor catalytic converter (UCC). This included evaluating TWC activity under realistic simulated exhaust conditions including fuel-rich, stoichiometric and fuel-lean ($0.99 \leq \lambda \leq 1.01$). Pt-substituted TWCs outperformed Pd-based counterparts, regardless of the converter type (WCC or UCC), in CO, C_3H_6 and C_3H_8 oxidation and NO reduction reactions under the simulated exhaust conditions tested. Moreover, Pt-substituted TWCs exhibited significant stability upon hydrothermal aging at 1,050 °C. The results show that after aging the Pt-substituted catalyst retained higher N_2 selectivity than the Pd-based TWC. Over Pd-based TWCs, N_2 selectivity drastically dropped from 70-80% to 15-35% after aging, while Pt-substituted TWCs N_2 selectivity dropped from 80-100% to only 60-80%. The key finding from this study is that Pt incorporation in a Pd/Rh TWC improves the emission control from gasoline vehicles in terms of both CO and HC oxidation and NO_x reduction.

Keywords: Three-Way Catalyst, Pt Substitution, Realistic Exhaust Gas Condition, Aging Effect, Emission Control

INTRODUCTION

Greenhouse gas (GHG) and fine particulate matter (PM) emissions are a great concern as they negatively impact climate change and human health. Vehicle emissions account for a considerable share of all pollutants in the atmosphere. In the latest IPCC AR6, the 2019 global anthropogenic GHG emissions were reported as 59 $GtCO_{2eq}$, of which 15% was attributed to transportation, and within this 70% was from road vehicles [1]. This means vehicle emission contributed roughly 6.2 $GtCO_{2eq}$, and the widespread global use of light-duty vehicles (LDVs) contributes a great deal to these emissions. LDVs emit nitrogen oxides (NO_x), carbon monoxide (CO) and unburned hydrocarbons (HCs) from internal engine combustion [2]. These exhaust pollutants are extremely hazardous to the environment and human health. Specifically, CO is a poisonous and harmful gas, HCs are greenhouse gases (particularly methane), and NO_x is a secondary source for PM formation [3]. To meet the legislated emissions regulations, gasoline vehicles utilize three-way catalytic converters (TWCs) to reduce emissions to acceptable levels. The TWC oxidizes CO and HCs to CO_2 and H_2O, while simultaneously reducing NO_x to N_2 [4,5]. The air-fuel ratio (λ) of the exhaust stream is an important factor for optimal TWC performance and should be maintained close to 1. At this value ($\lambda \approx 1$), the TWC can simultaneously convert CO, HCs and NO, and also control byproduct formation such as NH_3 and N_2O. NH_3 is a precursor to secondary atmospheric aerosols and reacts with nitrogen and ammonium nitrate to generate PM, which is harmful to human health [6]. Although N_2O accounts for only 7% of global GHG emissions, it has 300 times the greenhouse potential compared to CO_2. Ravishankara et al. stated that N_2O gas has contributed to the biggest im-

†To whom correspondence should be addressed.
E-mail: dkang@seoultech.ac.kr, melanie.hazlett@concordia.ca, sbkang@gist.ac.kr
‡These authors contributed equally.

pact on ozone depletion [7]. Thus, the scientific community developing TWCs must investigate the byproduct NH_3 and N_2O formation, how altering the engine operation to different λ values and temperatures can mitigate byproduct formation, and how altering the TWC formulation can reduce this byproduct formation [8,9].

The light-off temperatures of the reactants in the exhaust (LOTs or T_{50}: the temperature at which 50% conversion is observed) over TWCs is typically 250 °C to 300 °C; however, most exhaust gases are emitted before the TWC is fully warmed-up, referred to as cold-start emission [10,11]. Cold-start emission is a challenge to modern TWC development, since advanced engine technologies generally lead to lower exhaust temperatures, which exacerbates this problem [12]. Furthermore, N_2O and NH_3 are primarily released at lower LOTs (below 500 °C) [13,14]. Mainly, two types of catalytic converters have been installed in typical gasoline engine vehicles: a warm-up and an under-floor catalytic converter (WCC and UCC, respectively). The WCC is placed near the engine for high exhaust gas temperatures and is also identified as a function of the location (front and rear). The WCC front with relatively high PGM loading reduces pollutant emissions close to the engine, while the WCC rear with lower PGM loading plays a role in compensated aftertreatment after the WCC front. On the other hand, UCC is subjected to relatively lower temperatures due to its location further from the engine [15].

In general, platinum group metals (PGM) such as Pd, Rh and/or Pt have been used individually or together as active metals in the catalytic formulation of TWC. Each PGM exhibits distinct characteristics in the TWC activity. Specifically, Pd has a superior intrinsic activity for CO and HCs oxidation [16]. Pt is particularly effective in oxidizing saturated HCs, while Rh is highly active in the NO_x reduction compared to Pd and Pt [17]. For developing TWCs, the cost is a crucial factor as PGMs are generally expensive and the prices of Pd, Pt, and Rh have fluctuated significantly over the last decade. In past decades, there was a strong desire to replace Pt by the addition of Pd (Pt/Pd TWC) due to the higher price of Pt than Pd [18]. As a result, Ford introduced a Pd/Rh catalyst, in which Pt was replaced with Pd in 1989, despite its poisoning associated with lead and sulfur [19]. Additionally, a large number of studies for Pd/Rh-based TWC performance enhancement have been conducted [20-22]. As a result, as the Pd/Rh formulation improved over time, the choice of precious metals and loadings became more and more dependent on financial factors. However, in the last five years, the price of Pd has soared over Pt due to tremendous demand for Pd (Pd: 67.7 EUR/g and Pt: 28.1 EUR/g in 2020) [23]. Catalytic converter costs are heavily dependent on the PGM formulation. As a result of these recent price trends, modern TWC formulations are shifting back from Pd-based to Pt/Pd-based. Most studies on Pt/Pd-based TWCs merely discuss the effects of each PGM or the catalytic characteristics of various TWC formulations [24-27].

In this study, a comprehensive characterization of the impact of the Pt-substitution in Pd/Rh TWCs on the catalytic performance with respect to the air-to-fuel ratio (λ) and the aging behavior has been conducted. To investigate the contribution of Pt-substitution according to feed gas composition, six sets of commercial TWCs consisting of Pd/Rh, Pt/Rh and Pt/Pd/Rh formulations were systematically evaluated under each lean, rich and stoichiometric (ST) condition ($0.99 \leq \lambda \leq 1.01$). Based on these results, the influence of the Pt-substituted catalyst on emission control (NO, CO, HCs, NH_3 and N_2O emission) is discussed. Furthermore, the aging behavior of the TWCs with respect to the catalytic formulation was also examined by comparing the catalytic performance of fresh and aged catalysts, demonstrating that the Pt-substituted to Pd/Rh catalyst is the better catalytic formulation for improved N_2 selectivity in NO reduction.

Table 1. Commercial three-way catalysts (TWCs)

Sample	PGM loading (g/L)	PGM molar ratio		
		Pd	Pt	Rh
Pd-F[a]	9	25		1
Pd-R[b]	2	14		1
Pd-U[c]	2	2		1
PtPd-F[a]	9	18.75	6.25	1
PtPd-R[b]	2	10.5	3.5	1
Pt-U[c]	2		2	1

[a]WCC (warm-up catalytic converter) front
[b]WCC rear
[c]UCC (under-floor catalytic converter)

MATERIALS AND METHODS

1. Catalyst Sample

Six commercial TWCs used for light duty-gasoline engine vehicles are listed in Table 1 and were provided by Hyundai Motor R&D. These TWCs are WCC front, WCC rear and UCC. To investigate the effect of Pt-substitution to the catalytic formulation, the front and rear WCC systems are composed of Pd/Rh and Pd/Pt/Rh active metals, respectively, denoted as "Pd" for the Pd-based catalyst (Pd/Rh) and "PtPd" for the partially Pt-substituted in the Pd-based formulation (Pd/Pt/Rh). We also notate "-F" for the front and "-R" for the rear catalyst. The UCC system is comprised of Pd-based (Pd-U) and Pt-replaced (Pt-U) catalysts, while keeping the total molar ratio of PGM in counterpart catalysts. Note that all the Pd is substituted with Pt in this case. We tested both fresh and aged catalysts. The fresh catalysts were hydrothermally aged by the accelerated aging protocol with lean-rich periodic cycling containing 10% water vapor, which has been developed from Hyundai Motor R&D, at 1,050 °C for 30 h for the WCC and at 800 °C for 24 h for the UCC, respectively.

2. Catalyst Activity Test and Characterization

Aged TWC catalytic performance was evaluated in a packed bed reactor at 150,000 h^{-1} gas-hourly space velocity (GHSV), using 0.2 cc of crushed monolith samples sieved to 20-30 mesh size. The feed concentration listed in Table 2 was controlled using mass flow controllers. In addition, 10% water vapor was injected using a syringe pump, then vaporized in the pre-heater at the reactor inlet. Before each reactor test, the catalyst sample was pretreated at 500 °C for 1 h under the ST condition (λ=1) and then cooled to 100 °C in a N_2 flow. The steady-state catalytic activity was measured from 150 °C to 500 °C as a function of the A/F ratio (λ) of the simulated exhausts ranging from 0.99 (fuel-rich) to 1.01 (fuel-lean), defined as following Equation [28]:

Table 2. Simulated exhaust gas composition as a function of air-to-fuel ratio (fuel-rich: λ=0.99, stoichiometric: λ=1.00 and fuel-lean: λ=1.01)

Gas species	Unit	λ (A/F ratio)		
		Rich	Stoichiometric	Lean
		0.99	1.00	1.01
CO	ppm	7,200	6,000	4,200
H_2	ppm	2,400	2,000	1,400
O_2	ppm	5,000	6,000	7,000

*Other gases: 13.9% CO_2, 10% H_2O, 1,000 ppm NO, 444 ppm C_3H_6, 111 ppm C_3H_8 and N_2 balance

$$\lambda = \frac{1}{1+0.02545\{[H_2]+[CO]+(3n+1)[C_nH_{2n+2}]+3n[C_nH_{2n}]-[NO]-2[O_2]\}} \quad (1)$$

The concentrations of CO, NO, C_3H_6, C_3H_8, NH_3 and N_2O were analyzed using Fourier transform infrared spectroscopy (FTIR) gas analyzer (Perkin-Elmer Spectrum 2, Perkin-Elmer, USA) equipped with a long-path IR cell (5 m Long-Path Gas Cells, PIKE Technologies, USA). No NO_2 was measured, and thus the N_2 selectivity was determined from considering the NO, N_2O and NH_3 concentrations from the following equation:

$$N_2 \text{ selectivity } (\%) = \frac{[NO]_{inlet}-[NO]_{outlet}-[NH_3]_{outlet}-2[N_2O]_{outlet}}{[NO]_{inlet}-[NO]_{outlet}} \times 100 \quad (2)$$

X-ray photoelectron spectroscopy (XPS) analysis (NEXSA, Thermo Fisher Scientific) was also conducted to examine the chemical state of Pd3d of the PtPd-F and Pd-F. For all measurements, the binding energy observed by XPS was calibrated using 284.8 eV of surface adventitious C1s. The Shirley algorithm was used to determine the spectrum boundary condition.

RESULTS AND DISCUSSION

1. TWC Performance under Lean Exhaust Conditions

The six aged commercial TWCs, listed in Table 1, were evaluated under the fuel-lean condition (λ=1.01). The results for the CO, C_3H_6 and C_3H_8 oxidation and NO reduction are shown in Fig. 1, and the results for NH_3 and N_2O byproduct formation are shown in Fig. 3. The light-off temperatures of each reactant (LOTs or T_{50}; the temperature where the conversion reached 50%) are also summarized in Supplementary Information (Table S1). The Pt substitution over Pd-based catalysts affects oxidation performance for all oxidized species, CO, C_3H_6 and C_3H_8, as shown in Fig. 1(a)-(c). Particularly, for the WCC sample, the T_{50} for each component shifted to a lower temperature region compared to UCC sample. Comparing the Pd-F to PtPd-F samples, the T_{50} for CO, C_3H_6 and C_3H_8 decreased from 231, 277 and 436 °C to 228, 254 and 400 °C, respectively. The PtPd-R also exhibited lower T_{50}'s for CO and C_3H_6 compared to Pd-R from 284 and 322 °C for Pd-R and 270 to 286 °C for PtPd-R. Also, complete C_3H_6 conversion for PtPd-F and PtPd-R was attained at high temperature, which was not observed for the Pd-F and Pd-R catalysts. This enhanced oxidation performance of the Pt-substituted catalysts may be attributable to the Pt-Pd interaction [29]. As described in Fig. 2, we examined XPS analysis for PtPd-F and Pd-F to understand the impact of Pt-Pd interaction. Both catalysts have only one phase of Pd; however, it was present in the form of oxide in PtPd-F and metal in Pd-F. In detail, only

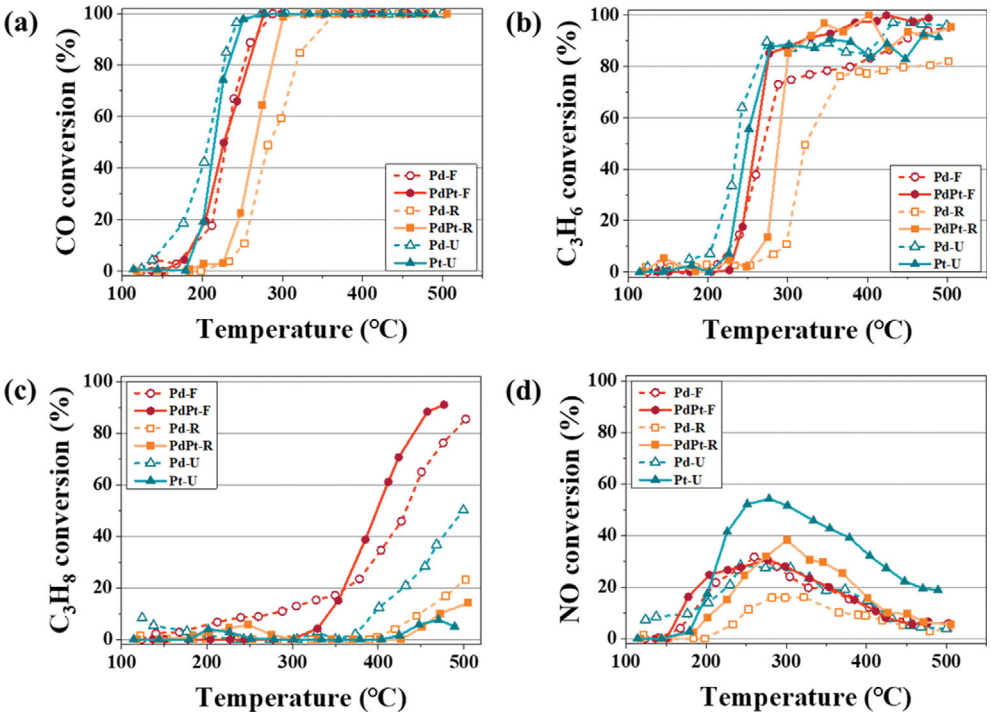

Fig. 1. (a) CO, (b) C_3H_6, (c) C_3H_8 and (d) NO conversion over TWCs under the fuel-lean condition (λ=1.01). Simulated fuel-lean exhaust: 4,200 ppm CO, 1,400 ppm H_2, 7,000 ppm O_2, 13.9% CO_2, 10% H_2O, 1,000 ppm NO, 444 ppm C_3H_6, 111 ppm C_3H_8 and N_2 balance.

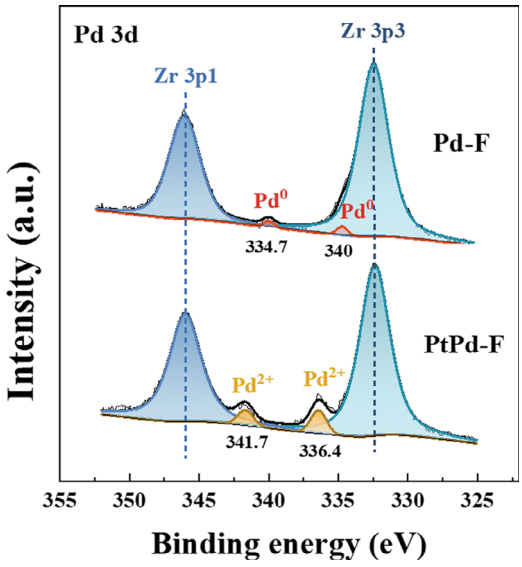

Fig. 2. XPS spectra of Pd3d over aged PtPd-F and Pd-F.

Pd3d oxide peak was observed for PtPd-F at 334.7 eV while Pd3d metal peak was only exhibited for Pd-F at 346 eV. Many studies have reported that the Pt-Pd bimetallic catalysts have a superior thermal stability compared to monometallic Pt-only and Pd-only due to the Pt-Pd interaction [30-32]. Therefore, we suggest that superior thermal stability is caused by converting the Pd phase to an oxide since Pd oxide is more active in oxidations than metallic Pd. Moreover, Pt^{4+} oxides formed on Pt/Pd catalysts provide more available sites for CO and HCs adsorptions with improved intrinsic oxidation activity, thus alleviating competitive oxidation between CO and HCs [33,34]. Consequently, as Pt is substituted, Pd maintained the oxide phase even after aging, resulting in a superior oxidation performance with Pt-substituted TWCs.

The effect of the Pt-substitution on the NO reduction performance was also evaluated and is shown in Fig. 1(d). Due to the higher oxygen concentration in the slightly fuel-lean condition (λ= 1.01), incomplete NO conversion is observed even at 500 °C. NO conversion was significantly enhanced over the PtPd-R and Pt-U. When comparing these to the Pd-R and Pd-U, the maximum NO

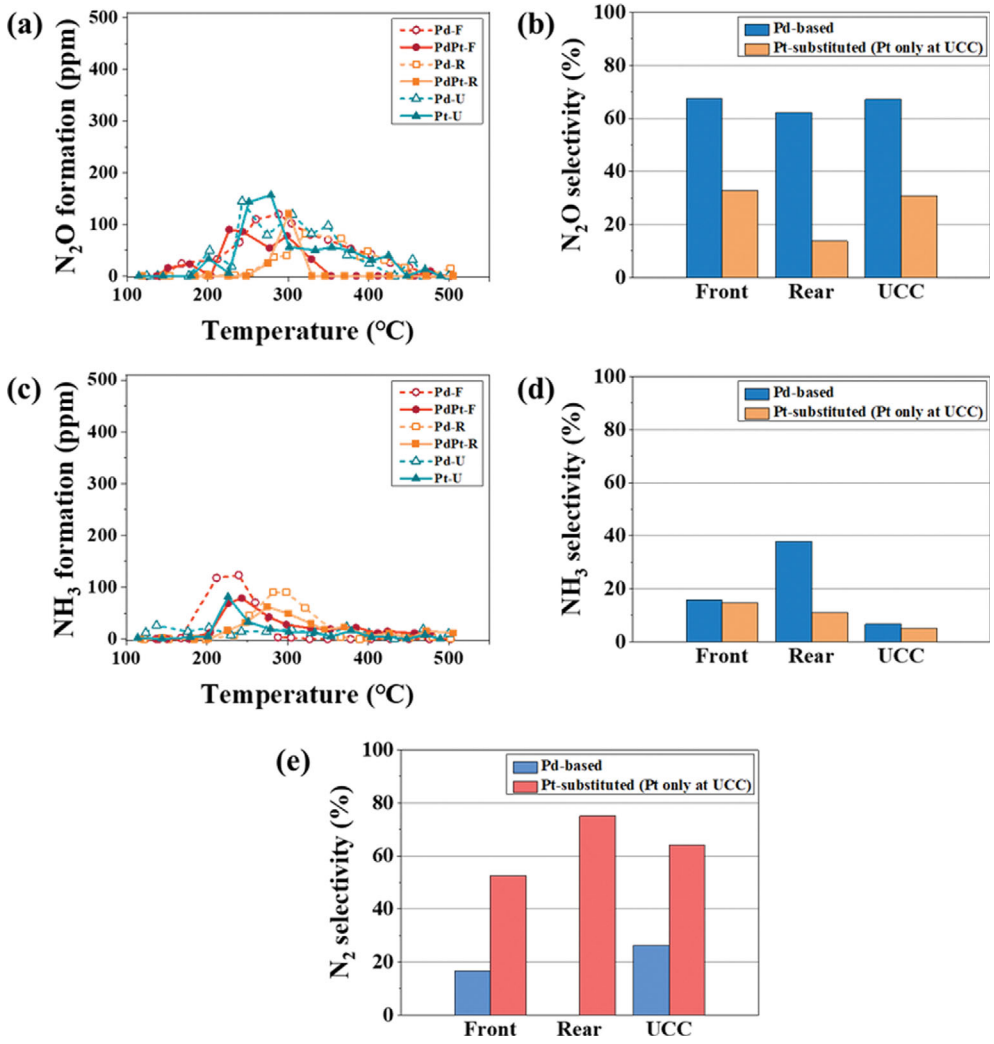

Fig. 3. N_2O and NH_3 emissions over aged TWCs under the fuel-lean condition (λ=1.01): (a) N_2O formation, (b) corresponding average N_2O selectivity, (c) NH_3 formation, (d) corresponding average NH_3 selectivity and (e) N_2 selectivity. Simulated fuel-lean exhaust: 4,200 ppm CO, 1,400 ppm H_2, 7,000 ppm O_2, 13.9% CO_2, 10% H_2O, 1,000 ppm NO, 444 ppm C_3H_6, 111 ppm C_3H_8 and N_2 balance.

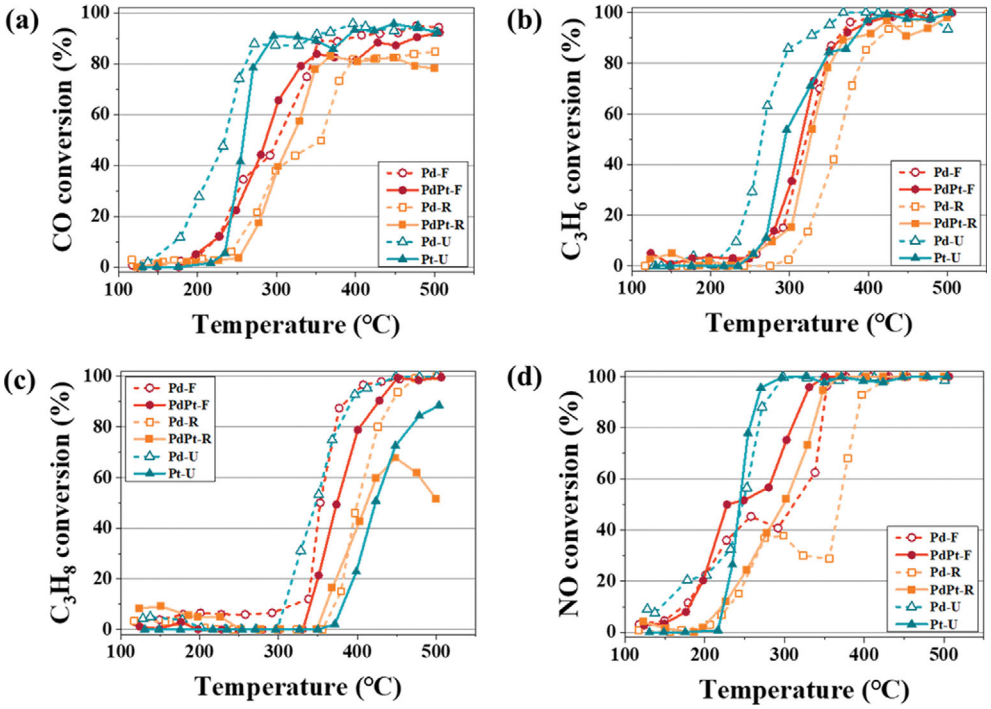

Fig. 4. (a) CO, (b) C_3H_6, (c) C_3H_8 and (d) NO conversion over aged TWCs under the fuel-rich condition (λ=0.99). Simulated fuel-rich exhaust: 7,200 ppm CO, 2,400 ppm H_2, 5,000 ppm O_2, 13.9% CO_2, 10% H_2O, 1,000 ppm NO, 444 ppm C_3H_6, 111 ppm C_3H_8 and N_2 balance.

conversion increased from 16% and 28% to 38% and 54%, respectively. This observation may be associated with the Pt-Rh interaction, which is more active in the NO reduction than the Pd-Rh interaction. Rh is an essential component in the NO reduction due to the superior reactivity of the NO-CO reaction [35]. In presence of Pt with Rh the metallic state of Rh is favored, which is active in the NO decomposition and the NO-CO reaction [36,37]. On the other hand, the presence of PdO together with Rh on the surface induces the formation of Pd/Rh alloy upon thermal aging, which is inactive for NO conversion [17,38].

The N_2O and NH_3 byproduct formation over the various catalyst formulations is shown in Fig. 3. There is not a large difference observed in the maximum N_2O formation, where Pd-F, Pd-R and Pd-U emitted 119, 82 and 119 ppm of N_2O, and PtPd-F, PtPd-R and Pt-U emitted similar levels with 90, 121 and 157 ppm, respectively. However, looking at the average N_2O emissions over the entire temperature range, the Pt-substituted TWCs exhibit a clear benefit over the entire temperature range measured when compared to the Pd-based catalysts. As shown in Fig. 3(b), the average N_2O selectivity from the NO conversion significantly decreased by the Pt-substitution from 60% to 30%, regardless of converter type (WCC front, WCC rear and UCC). The decrease in the N_2O selectivity is due in part to the higher ability to dissociate N_2O on Pt sites, meaning in turn that N_2O formation is less favorable [39]. These results indicate that the presence of Pt in the TWC formulation is essential to control N_2O emissions.

For NH_3 formation, the Pt-substituted catalysts are also beneficial to reducing NH_3 emissions in terms of the maximum level and its average value. As shown in Fig. 3(d), the average level of the NH_3 selectivity decreased by the Pt-substitution, particularly for the WCC rear. The NH_3 selectivity is lower than that of N_2O regardless of the catalysts employed, suggesting that the major byproduct formation pathway is NO conversion to N_2O rather than NH_3 under the fuel-lean condition. N_2O is mainly produced under lean conditions, and the corresponding selectivity of N_2O can be lowered by the Pt substitution. Consequently, the deNOx to N_2 activity of Pt-substituted catalysts is superior to that of Pd-based catalysts (Fig. 3(e)).

2. TWC Performance under Rich Exhaust Conditions

The TWC performance under the fuel-rich condition (λ=0.99) was also evaluated as shown in Fig. 4 comparing oxidation and reduction performance and Fig. 5 comparing N_2O and NH_3 byproduct formation. Fig. 4 shows that the PtPd-F and PtPd-R catalysts outperformed Pd-based counterparts in oxidizing CO and C_3H_6 (Fig. 4(a) and Fig. 4(b)), which was also observed in the fuel-lean condition as discussed earlier. Comparing the Pd-F and Pd-R, the T_{50} of CO and C_3H_6 over PtPd-F and PtPd-R shifted to lower temperatures from 301 to 287 °C and 358 to 316 °C, respectively, as listed in Table S1. This implies the Pt-substitution in Pd-based TWC formulation can achieve a superior oxidation activity for CO and C_3H_6 under both fuel-lean and -rich conditions. It can also be observed that there is no plateau or step in the light-off curve for CO oxidation over Pt-substituted catalysts compared to Pd-based. However, in Fig. 4(c), the addition of Pt negatively impacts the C_3H_8 oxidation performance by shifting the T_{50} to higher temperatures. For the NO conversion in Fig. 4(d), the Pt-substituted catalysts also show earlier NO light-off and lower temperatures required for complete NO conversion than their Pd-based counterparts. When comparing the UCC system, the Pt-U without Pd in the formulation exhibits inferior oxidation activity CO, C_3H_6 and C_3H_8 compared to the

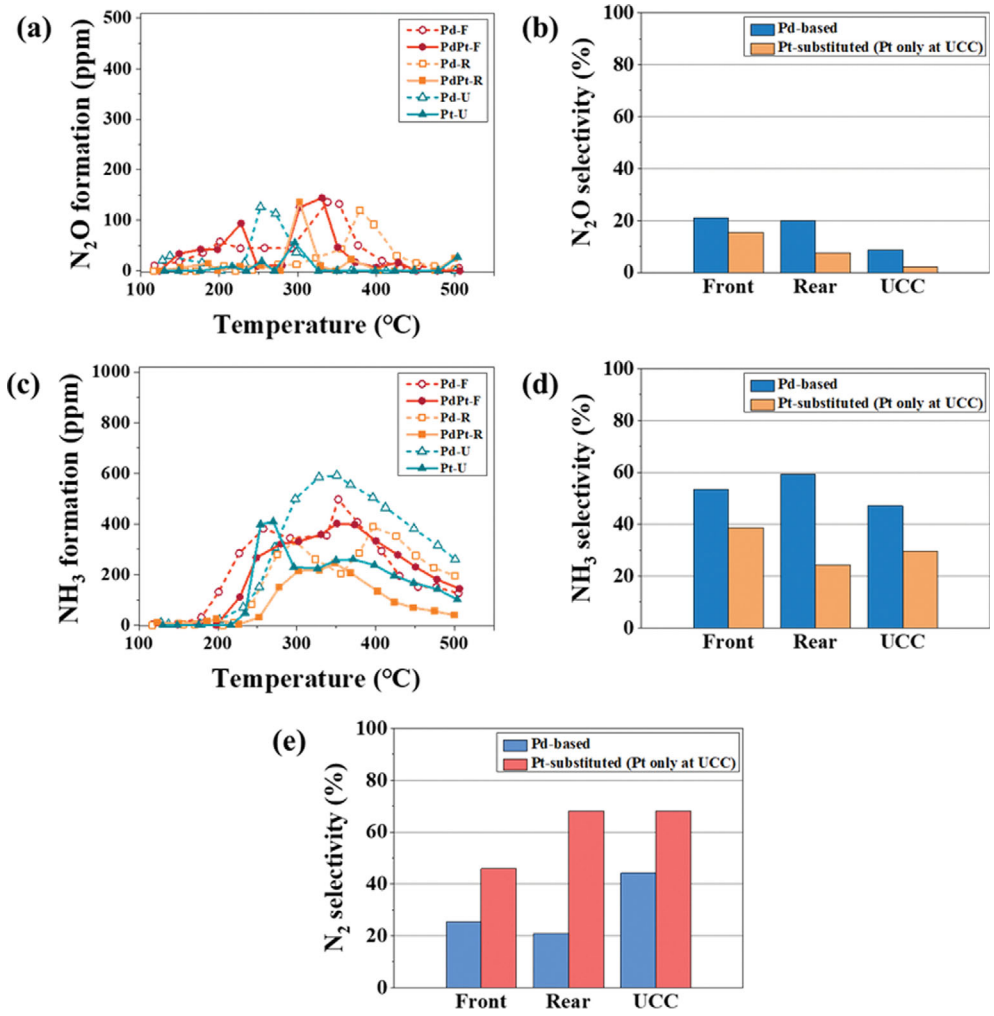

Fig. 5. N_2O and NH_3 emissions over aged TWCs under the fuel-rich condition (λ=0.99): (a) N_2O formation, (b) corresponding average N_2O selectivity, (c) NH_3 formation, (d) corresponding average NH_3 selectivity and (e) N_2 selectivity. Simulated fuel-rich exhaust: 7,200 ppm CO, 2,400 ppm H_2, 5,000 ppm O_2, 13.9% CO_2, 10% H_2O, 1,000 ppm NO, 444 ppm C_3H_6, 111 ppm C_3H_8 and N_2 balance.

Pd-U. This may be attributed to the high activity of Pd in water gas shift (WGS: $CO+H_2O \rightarrow CO_2+H_2$) and steam reforming (SR: $C_nH_m+nH_2O \rightarrow nCO+(m/2+n)H_2$), which occurs under the oxygen-deficient condition (fuel rich) [40]. Note that Pt was partially substituted in the Pd/Rh WCC system, while the UCC system was comprised of Pd/Rh and Pt/Rh (instead of Pd) catalysts, as listed in Table 1.

The N_2O and NH_3 emission behavior in Fig. 5(a) and Fig. 5(b), respectively, demonstrates that Pt-substitution into the catalyst formulation reduces N_2O and NH_3 byproduct formation, indicating high N_2 selectivity as shown in Fig. 5(e). In fuel-rich conditions, the preferred byproduct of NO reduction was observed to be NH_3 rather than N_2O. The opposite trend was observed in the fuel-lean condition. Since the fuel-rich condition is oxygen-deficient relative to the amount of reductants such as CO, H_2 and HCs, the higher level of NH_3 formation than N_2O may be due to the catalytic surface reactions involving H_2 from SR and WGS, thereby more apparently proceeding the NO-H_2 pathway to NH_3 formation [41,42] rather than the NO-CO pathway. Thus, the high NO conversion of Pt-substituted catalysts is due to a possible reaction pathway, internal selective catalytic reduction (SCR) reaction ($NO+NH_3 \rightarrow N_2+H_2O$), with surface NH_3 readily formed by NO-H_2 and NO-HC reactions [46]. Under both non-stoichiometric conditions, the presence of Pt together with Pd/Rh clearly improves the N_2 selectivity during the course of the NO reduction, mitigating N_2O and/or NH_3 formations.

3. TWC Performance under Stoichiometric Exhaust Condition

The conversions of CO, C_3H_6, C_3H_8 and NO were also compared with respect to Pt-substituted and Pd-based aged catalysts under the ST condition (λ=1.00), as presented in Fig. 6. Superior catalytic performance was also observed over Pt-substituted catalysts compared to Pd-based catalysts under the ST condition. For the WCC front brick, the PtPd-F dramatically outperformed the Pd-F with lower T_{50} of CO, HCs and NO conversion. The T_{50} values for CO, C_3H_6, C_3H_8 and NO decreased by 11, 55, 56 and 159 °C, respectively, with the Pt-substitution. In addition, a similar trend was observed for the WCC rear brick when comparing the Pd-R and PtPd-R catalysts. The Pt-substitution led to a decrease in the

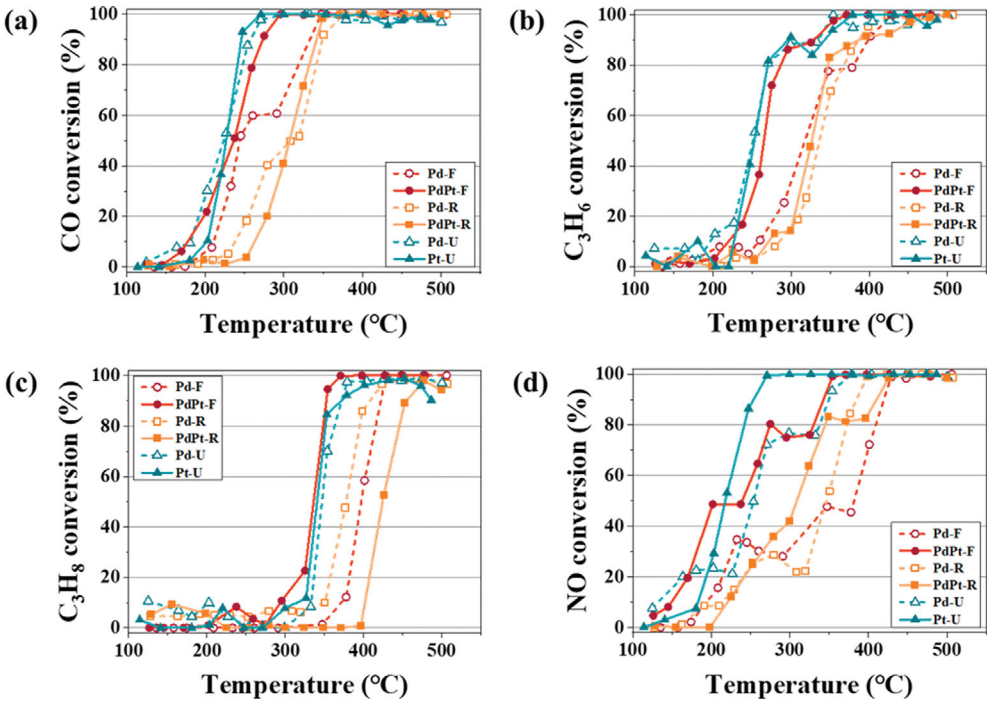

Fig. 6. (a) CO, (b) C_3H_6, (c) C_3H_8 and (d) NO conversion over aged TWCs under the stoichiometric condition (λ=1.00). Simulated stoichiometric exhaust: 6,000 ppm CO, 2,000 ppm H_2, 6,000 ppm O_2, 13.9% CO_2, 10% H_2O, 1,000 ppm NO, 444 ppm C_3H_6, 111 ppm C_3H_8 and N_2 balance.

T_{50} values for CO, C_3H_6 and NO by 5, 8, and 37 °C, respectively. However, in this case the C_3H_8 T_{50} value increased by 46 °C, consistent with the fuel-rich and fuel-lean results. For the UCC brick, Pt-U and Pd-U show comparable T_{50} values of CO and HCs, where Pt-U achieves earlier light-off of NO than Pd-U by 36 °C. N_2O and NH_3 formation during NO reduction for ST condition is shown in Fig. 7. Consistent with the fuel-lean and fuel-rich results, the ST results show the impact of Pt-substitution and presence of Pt in the formulation on mitigating by-product emissions. Comparing the average N_2O selectivity over WCC catalysts in Fig. 7(b), the PtPd-F and PtPd-R emitted significantly less N_2O compared to Pd-F and Pd-R, respectively, over the temperature range studied. Moreover, Pt-U had only 18% N_2O selectivity compared to Pd-U with 35% N_2O selectivity. From Fig. 7(c)-(d), it is observed that the NH_3 emissions can also be effectively controlled with the Pt-substituted catalysts. The average NH_3 selectivity of the Pt-substituted catalysts, PtPd-F (12%) and PtPd-R (16%), is lower compared to the Pd samples, Pd-F (41%) and Pd-R (31%). This again indicates that Pt-containing TWCs (PtPd-F, PtPd-R and Pt-U) shows high N_2 selectivity compared to Pd-based (Pd-F, Pd-R and Pd-U) as shown in Fig. 7(e). The Pt-substitution to Pd-based TWC comprehensively exhibits a positive impact on converting exhaust components such as CO, HCs and NO and reducing N-related byproducts such as NH_3 and N_2O emissions, regardless of the exhaust conditions, as also summarized in Table S1.

4. Aging Performance of Pt-substituted TWC

Catalyst thermal stability is also a crucial factor in determining the optimal catalytic formulation; thus we also compared fresh catalysts to aged counterparts with respect to the exhaust conditions. Note that Fig. S1 provides the light-off curves of reactants and by-product formation over the fresh catalysts. Focusing on the NO conversion and corresponding N_2 selectivity in Fig. 8 for the ST condition, Pt-substituted TWCs reveal a significant durability upon the thermal aging, exhibiting smaller decreases in both NO conversion and N_2 selectivity than observed for the Pd-based catalysts. The Pd-based catalysts exhibit significant deactivation upon the thermal aging compared to the Pt-substituted ones. On the Pd-based catalysts the NO conversion drastically drops from 70-90% to 30-45%, and the N_2 selectivity is also significantly decreased from 70-80% to 15-35% by the aging. On the other hand, TWCs N_2 selectivity drops from 80-100% to only 60-80%. When Pt coexists with Pd and Rh, the thermal stability enhancement has been related to the formation of Pt-Pd crystallites, compared to monometallic Pt or Pd catalysts [29,43].

The overall TWC performance comparison of fresh and aged catalysts is presented in Fig. 9. The LOTs for the various exhaust components (CO, HCs and NO) and the N_2 selectivity for the WCC-F, WCC-R, and UCC for each of Pt-substituted and Pd-based catalysts are plotted against each other for easy comparison. First, CO LOTs are higher over Pd-based TWCs compared to Pt-substituted catalysts in most tested conditions (Fig. 9(a)). That is, commercial Pt-substituted TWCs effectively convert CO with lower temperature range over both fresh and aged catalysts. Specifically, Pt-substituted catalysts show lower LOTs, and the maximum gaps of T_{50} and T_{90} were 42 and 129 °C, respectively, showing that full conversion is reached at lower temperatures after light-off. Secondly, LOTs of HCs including C_3H_6 and C_3H_8 show no particular tendency (Fig. 9(b)). This can be explained by the fact that the WGS and SR

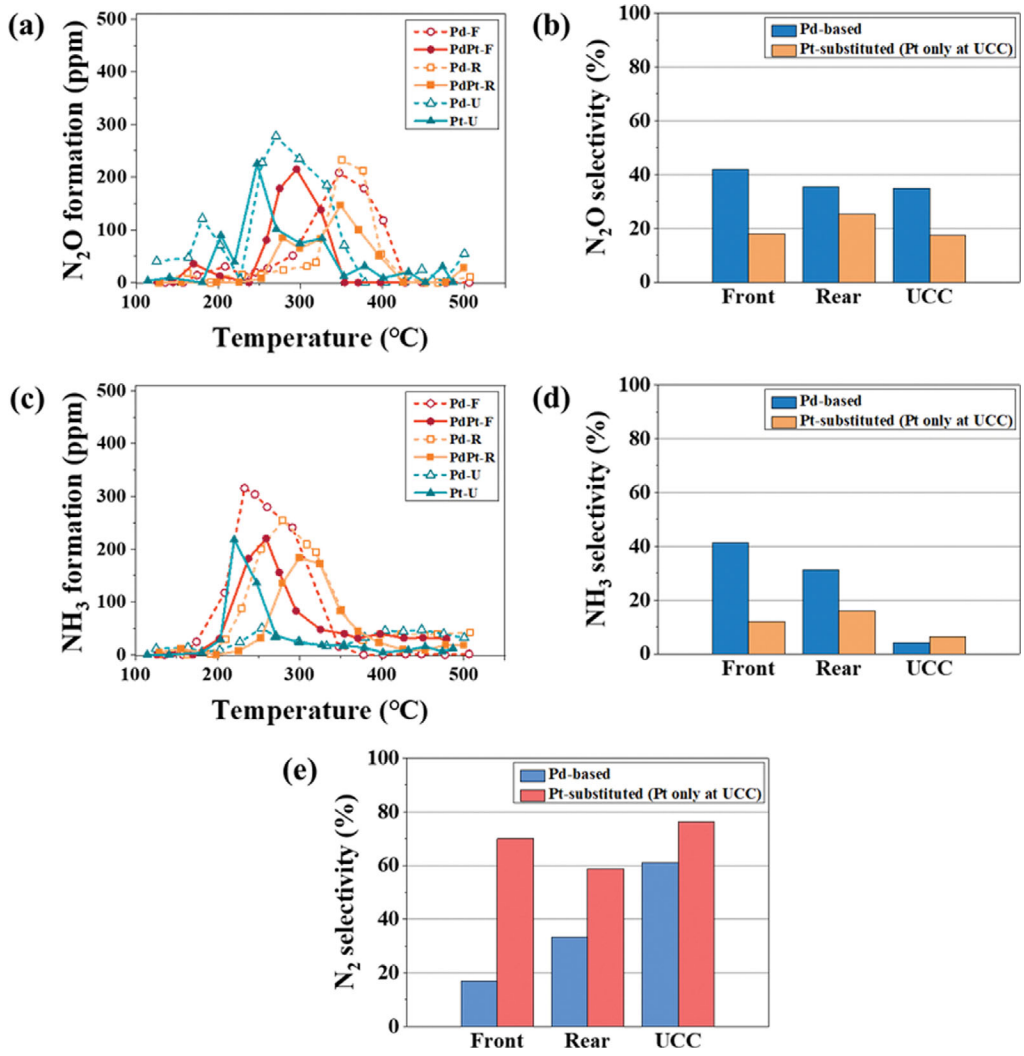

Fig. 7. N_2O and NH_3 emissions over aged TWCs under the stoichiometric condition (λ=1.00): (a) N_2O formation, (b) corresponding average N_2O selectivity, (c) NH_3 formation, (d) corresponding average NH_3 selectivity and (e) N_2 selectivity. Simulated stoichiometric exhaust: 6,000 ppm CO, 2,000 ppm H_2, 6,000 ppm O_2, 13.9% CO_2, 10% H_2O, 1,000 ppm NO, 444 ppm C_3H_6, 111 ppm C_3H_8 and N_2 balance.

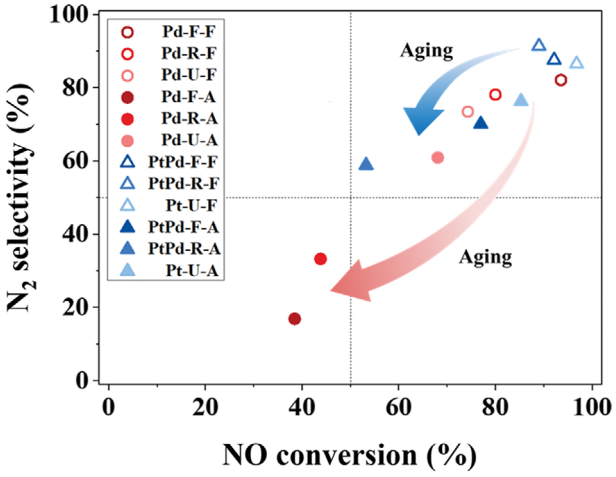

Fig. 8. Aging performance in averaged N_2 selectivity and NO conversion comparing fresh and aged TWCs under the stoichiometric condition.

reactions are more active than NO-CO or NO-HCs reaction over Pd-based TWCs as mentioned in Section 3.1. Regarding NO LOTs, lower LOTs are observed over both fresh and aged Pt-substituted catalysts in most conditions (Fig. 9(c)). Specifically, T_{50} of Pt-substituted catalysts are 6-159 °C lower than Pd-based catalysts for most conditions. Finally, the corresponding averaged N_2 selectivity shows the superior performance of Pt-substituted catalysts (Fig. 9(d)). Note that the average N_2 selectivity was obtained from the data in the range of 200-400 °C in which there was N_2O or NH_3 formation during the NO conversion. Over the both fresh and aged Pt-substituted TWCs show higher N_2 selectivity than Pd-based catalysts. The maximum N_2 selectivity over aged Pt-substituted TWCs is 19% higher than that over aged Pd-based TWCs. This reveals that H_2 generated through WGS and SR reactions over Pd, which was dominant in rich condition, was greatly involved in the higher NH_3 formation and resulted in lower N_2 selectivity. The Pt-substituted TWCs overall exhibit a superior performance abating NO with highly selective N_2 emission.

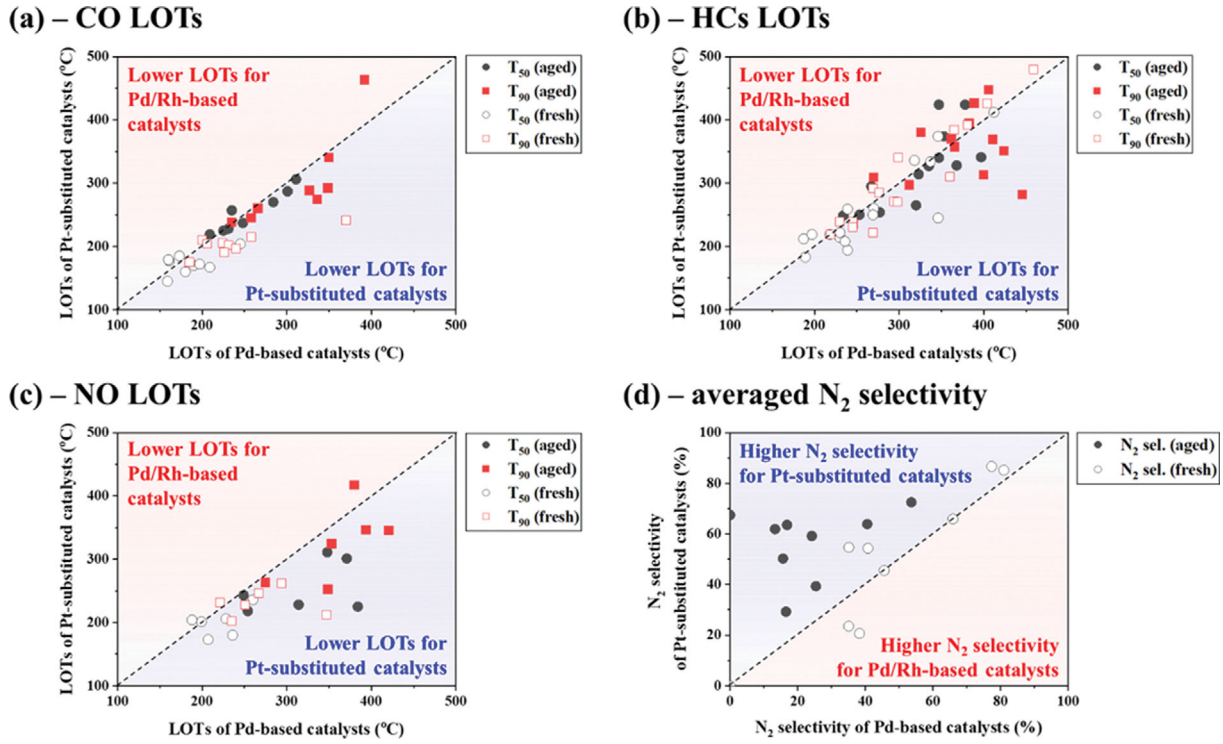

Fig. 9. Comprehensive performance of fresh and aged TWCs in LOTs (T_{50} and T_{90}) of (a) CO, (b) HCs, (c) NO and (d) averaged N_2 selectivity under cold start stage with respect to exhaust condition (λ=1.01, 1.00 and 0.99, respectively).

CONCLUSIONS

The effect of Pt-substitution on emission control was investigated through measuring comprehensive TWC performance (oxidation, reduction and selectivity). Various three-way catalysts (TWCs) were systematically evaluated focusing on the effect of Pt-substitution with respect to the converter type (WCC-F, WCC-R and UCC) and exhaust environments (fuel-lean, stoichiometric and fuel-rich). The TWC performance was assessed by comparing the CO, HCs and NO conversion and the N_2O, NH_3 and N_2 selectivity for six aged commercial TWCs under various feed gas composition ($0.99 \leq \lambda \leq 1.01$). Under the lean condition, where the N_2O formation is predominant during NO reduction, N_2O selectivity is impressively minimized through Pt-substitution with NO conversion at lower temperature and CO and HCs conversions are highly enhanced over aged Pt-substituted catalysts. The improved TWC performance was also examined under fuel-rich condition, where NH_3 is the main NO reduction by-product, Pt-substituted TWCs exhibited superior NO conversion and corresponding N_2 selectivity compared to Pd-based TWCs.

The TWC performance under the stoichiometric condition also confirmed that enhanced CO, HCs and NO conversion and selectivity performance can be achieved by Pt-substitution. Specifically, the data showed that Pt-substitution could promote both CO and HCs oxidation and NO reduction, resulting in the superior N_2 selectivity. It was also found that the Pt-substituted TWCs are also much more durable upon the thermal aging than their Pd-based counterparts. Finally, simultaneously comparing the NO conversion and corresponding N_2 selectivity usefully provides a guideline for improved TWC formulation with a small substitution of Pt in Pd-based catalysts. In summary, this PGM formulation (Pt-substituted on Pd-Rh TWC) is promising TWCs for reducing emissions from gasoline engines.

ACKNOWLEDGEMENTS

This work is supported by Hyundai Motor Company, National Research Foundation of Korea (NRF) Grant funded by the Korean government (MSIT) (No. 2021R1C1C1005404 and No. 2021R1 A5A1028138), GIST Research Institute (GRI) grant funded by the GIST in 2023.

AUTHOR CONTRIBUTIONS

D. Y. K.: data curation, formal analysis, investigation, software, writing original draft. W. B. B.: data curation, formal analysis, investigation, methodology, writing original draft. S. W. B.: data curation, formal analysis. M. J. H.: data curation, writing - review & editing, formal analysis. D. Y. Y.: resources, formal analysis. C. J.: resources, formal analysis. C. H. K.: resources, formal analysis. D. K.: supervision, writing - review & editing. S. B. K.: conceptualization, funding acquisition, project administration, supervision, writing - review & editing. All authors have read and agreed to the published version of the manuscript.

CONFLICT OF INTEREST

The authors declare that they have no known competing finan-

cial interests or personal relationships that could have appeared to influence the work reported in this paper.

SUPPORTING INFORMATION

Additional information as noted in the text. This information is available via the Internet at http://www.springer.com/chemistry/journal/11814.

REFERENCES

1. T. P. Kobylinski and B. W. Taylor, *J. Catal.*, **33**, 376 (1974).
2. A. Winkler, P. Dimopoulos, R. Hauert, C. Bach and M. Aguirre, *Appl. Catal. B*, **84**, 162 (2008).
3. R. Prasad and P. Singh, *Catal. Rev.*, **54**, 224 (2012).
4. M. Salaün, A. Kouakou, S. Da Costa and P. Da Costa, *Appl. Catal. B*, **88**, 386 (2009).
5. M. Haneda, K. Shinoda, A. Nagane, O. Houshito, H. Takagi, Y. Nakahara, K. Hiroe, T. Fujitani and H. Hamada, *J. Catal.*, **259**, 223 (2008).
6. P. Nevalainen, N. M. Kinnunen, A. Kirveslahti, K. Kallinen, T. Maunula, M. Keenan and M. Suvanto, *Appl. Catal. A*, **552**, 30 (2018).
7. A. R. Ravishankara, J. S. Daniel and R. W. Portmann, *Science*, **326**, 123 (2009).
8. J. Gao, H. Chen, Y. Liu, J. Laurikko, Y. Li, T. Li and R. Tu, *Sci. Total Environ.*, **801**, 149789 (2021).
9. M. Takei, H. Matsuda, Y. Itaya, S. Deguchi, K. Nakano, K. Nagahashi, M. Yoshino, J. Shibata and M. Hasatani, *Fuel*, **77**, 1027 (1998).
10. M. Skoglundh and E. Fridell, *Top. Catal.*, **28**, 79 (2004).
11. R. Tu, J. Xu, A. Wang, Z. Zhai and M. Hatzopoulou, *Sci. Total Environ.*, **760**, 143402 (2021).
12. G. Sathish Sharma, M. Sugavaneswaran and R. Prakash, *Fuel*, **309**, 122146 (2022).
13. I. Mejía-Centeno and G. A. Fuentes, *Chem. Eng. Commun.*, **196**, 1140 (2009).
14. N. W. Cant, D. E. Angove and D. C. Chambers, *Appl. Catal. B*, **17**, 63 (1998).
15. I. Heo, J. W. Choung, P. S. Kim, I.-S. Nam, Y. I. Song, C. B. In and G. K. Yeo, *Appl. Catal. B*, **92**, 114 (2009).
16. J. Wang, H. Chen, Z. Hu, M. Yao and Y. Li, *Catal. Rev.*, **57**, 79 (2014).
17. M. Shelef and G. W. Graham, *Catal. Rev.*, **36**, 433 (1994).
18. N. R. Collins and M. V. Twigg, *Top. Catal.*, **42**, 323 (2007).
19. M. Shelef and R. W. McCabe, *Catal. Today*, **62**, 35 (2006).
20. W.-J. Li and M.-Y. Wey, *Sci. Total Environ.*, **707**, 136137 (2020).
21. A. A. Vedyagin, M. S. Gavrilov, A. M. Volodin, V. O. Stoyanovskii, E. M. Slavinskaya, I. V. Mishakov and Y. V. Shubin, *Top. Catal.*, **56**, 1008 (2013).
22. V. Papadakis, C. Pliangos, I. Yentekakis, X. Verykios and C. Vayenas, *Catal. Today*, **29**, 71 (1996).
23. E. Vasile, A. Ciocanea, V. Ionescu, I. Lepadatu, C. Diac and S. N. Stamatin, *Ultrason. Sonochem.*, **72**, 105404 (2021).
24. B. Engler, E. Lox, K. Ostgathe, T. Ohata, K. Tsuchitani, S. Ichihara, H. Onoda, G. Garr and D. Psaras, *SAE Technical Paper*, 940928 (1994).
25. J. Cooper and J. Beecham, *Plat. Met. Rev.*, **57**, 281 (2013).
26. J. Jeong, B. Choi, M. Jung and G. Son, *SAE Technical Paper*, 2003-01-1873 (2003).
27. J. G. Nunan, W. B. Williamson, H. J. Robota and M. G. Henk, *SAE Transactions*, **104**, 310 (1995).
28. J. R. González-Velasco, J. A. Botas, J. A. González-Marcos and M. A. Gutiérrez-Ortiz, *Appl. Catal. B*, **12**, 61 (1997).
29. P. H. Ho, J. Shao, D. Yao, R. F. Ilmasani, M. A. Salam, D. Creaser and L. Olsson, *J. Environ. Chem. Eng.*, **10**, 108217 (2022).
30. J. Kim, Y. Kim, M. H. Wiebenga, S. H. Oh and D. H. Kim, *Appl. Catal. B*, **251**, 283 (2019).
31. S. B. Kang, M. Hazlett, V. Balakotaiah, C. Kalamaras and W. Epling, *Appl. Catal. B*, **223**, 67 (2018).
32. M. J. Hazlett, M. Moses-Debusk, J. E. Parks, L. F. Allard and W. S. Epling, *Appl. Catal. B*, **202**, 404 (2017).
33. F. Grasset, P. Alphonse, C. Labrugère, J. Darriet and A. Rousset, *Mater. Res. Bull.*, **34**, 2101 (1999).
34. T. Montanari, R. Matarrese, N. Artioli and G. Busca, *Appl. Catal. B*, **105**, 15 (2011).
35. K. Taylor, *J. Catal.*, **63**, 53 (1980).
36. Z. Hu, *Chem. Commun.*, **4**, 879 (1996).
37. Z. Hu, F. M. Allen, C. Z. Wan, R. M. Heck, J. J. Steger, R. E. Lakis and C. E. Lyman, *J. Catal.*, **174**, 13 (1998).
38. X. Liu, J. Chen, G. Zhang, Y. Wu, P. Shen, L. Zhong and Y. Chen, *J. Environ. Chem. Eng.*, **9**, 105570 (2021).
39. P. Granger, C. Dujardin, J. F. Paul and G. Leclercq, *J. Mol. Catal. A Chem.*, **228**, 241 (2005).
40. B. I. Whittington, C. J. Jiang and D. L. Trimm, *Catal. Today*, **26**, 41 (1995).
41. N. Le Phuc, X. Courtois, F. Can, S. Royer, P. Marecot and D. Duprez, *Appl. Catal. B*, **102**, 362 (2011).
42. Y. Liu, H. Wang, N. Li, J. Tan and D. Chen, *Sci. Total Environ.*, **795**, 148926 (2021).
43. J. Schütz, H. Störmer, P. Lott and O. Deutschmann, *Catalysts*, **11**, 300 (2021).

Supporting Information

Pt substitution in Pd/Rh three-way catalyst for improved emission control

Do Yeong Kim[*,‡], Wo Bin Bae[*,‡], Sang Woo Byun[*], Young Jin Kim[**], Dal Young Yoon[***], Changho Jung[***], Chang Hwan Kim[***], Dohyung Kang[**,†], Melanie J. Hazlett[*****,†], and Sung Bong Kang[*,†]**

*Research Center for Innovative Energy and Carbon Optimized Synthesis for Chemicals (Inn-ECOSysChem) and School of Earth Sciences and Environmental Engineering, Gwangju Institute of Science and Technology, 123 Cheomdangwagi-ro, Gwangju 61005, Korea

**Center for Environment & Sustainable Resources, Korea Research Institute of Chemical Technology (KRICT), 141 Gajeong-ro, Daejeon 34114, Korea

***Energy & Environmental Chemical Systems Lab, IFAT (Institute of Fundamental & Advanced Technology), R&D Division, Hyundai Motor Company, 37, Cheoldobagmulgwan-ro, Uiwang-si, Gyeonggi-do 16082, Korea

****Department of Future Energy Convergence, Seoul National University of Science and Technology, 232 Gongreung-ro, Nowon-gu, Seoul 01811, Korea

*****Chemical and Materials Engineering, Gina Cody School of Engineering and Computer Science, Concordia University, Montreal, QC, H4B1R6, Canada

(*Received 10 December 2022 • Revised 8 February 2023 • Accepted 9 February 2023*)

Table S1. Light-off temperatures (temperature at 50% conversion) for CO, C_3H_6, C_3H_8 and NO over commercial aged TWCs

Catalyst	CO T_{50} (°C)			C_3H_6 T_{50}(°C)			C_3H_8 T_{50} (°C)			NO T_{50} (°C)		
	Lean	ST	Rich	Lean	ST	Rich	Lean	ST	Rich	Lean	ST	Rich
Pd-F	231	248	301	277	320	323	436	397	353	*n.d.	384	314
PtPd-F	228	237	287	254	265	314	400	341	374	*n.d.	225	228
Pd-R	284	311	358	322	335	368	*n.d.	378	399	*n.d.	348	371
PtPd-R	270	306	316	286	327	328	*n.d.	424	410	*n.d.	311	300
Pd-U	209	225	235	234	253	267	500	347	347	*n.d.	254	249
Pt-U	219	225	257	249	250	295	*n.d.	340	424	238	218	243

*n.d.: not determined (relevant conversions are less than 50%)

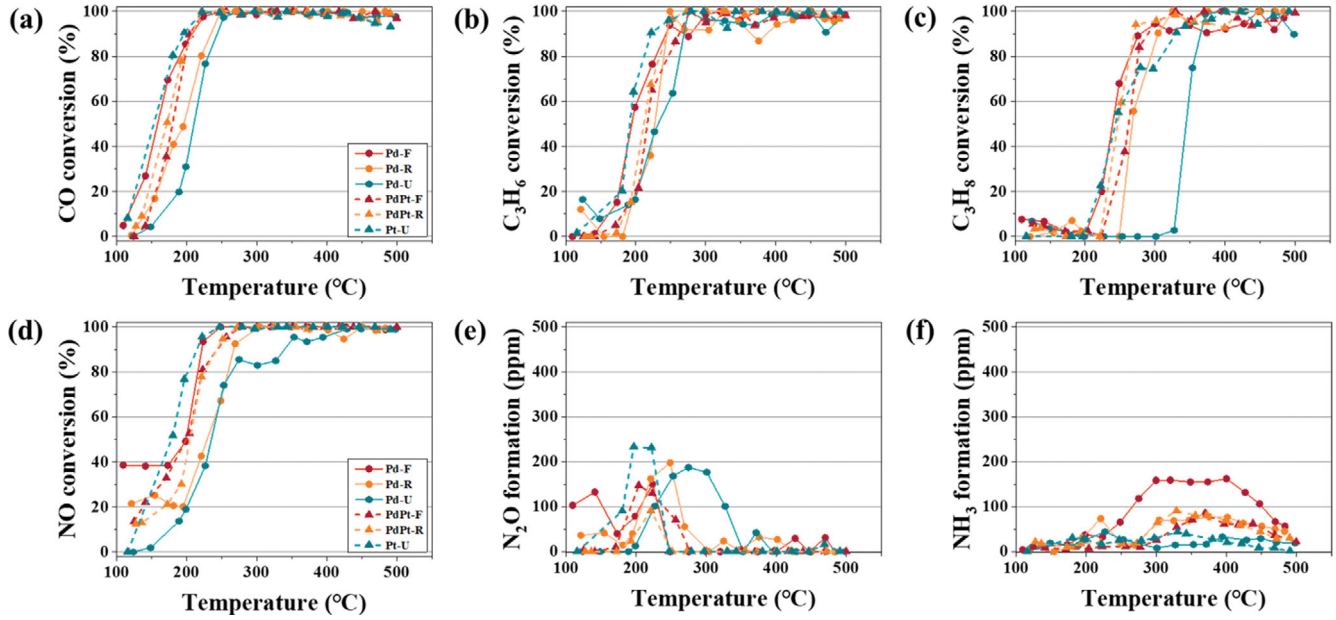

Fig. S1. Catalytic performance of fresh TWCs under the stoichiometric condition (λ=1.00) for (a) CO, (b) C_3H_6, (c) C_3H_8 and (d) NO conversion, and byproduct formation of (e) NH_3 and (f) N_2O.